Computers, Materials & Continua CMC, vol.65, no.3, pp.2009-2032, 2020

A Systematic Molecular Dynamics Investigation on the Graphene Polymer Nanocomposites for Bulletproofing

Hamidreza Noori[1], Bohayra Mortazavi[2, 3], Alessandro Di Pierro[4], Emad Jomehzadeh[5], Xiaoying Zhuang[2, 3], Zi Goangseup[6], Kim Sang-Hyun[7] and Timon Rabczuk[8, 9, *]

Abstract: In modern physics and fabrication technology, simulation of projectile and target collision is vital to improve design in some critical applications, like; bulletproofing and medical applications. Graphene, the most prominent member of two dimensional materials presents ultrahigh tensile strength and stiffness. Moreover, polydimethylsiloxane (PDMS) is one of the most important elastomeric materials with a high extensive application area, ranging from medical, fabric, and interface material. In this work we considered graphene/PDMS structures to explore the bullet resistance of resulting nanocomposites. To this aim, extensive molecular dynamic simulations were carried out to identify the penetration of bullet through the graphene and PDMS composite structures. In this paper, we simulate the impact of a diamond bullet with different velocities on the composites made of single- or bi-layer graphene placed in different positions of PDMS polymers. The underlying mechanism concerning how the PDMS improves the resistance of graphene against impact loading is discussed. We discuss that with the same content of graphene, placing the graphene in between the PDMS result in enhanced bullet resistance. This work comparatively examines the enhancement in design of polymer nanocomposites to improve their bulletproofing

[1] Institute of Structural Mechanics, Bauhaus-Universität Weimar, Weimar, D-99423, Germany.

[2] Chair of Computational Science and Simulation Technology, Department of Mathematics and Physics, Leibniz Universität Hannover, Hannover, 30157, Germany.

[3] Cluster of Excellence PhoenixD (Photonics, Optics, and Engineering-Innovation Across Disciplines), Gottfried Wilhelm Leibniz Universität Hannover, Hannover, Germany.

[4] Dipartimento di ScienzaApplicata e Tecnologia, Politecnico di Torino, Alessandria Campus, Alessandria, 15121, Italy.

[5] Faculty of Mechanical and Material Engineering, Graduate University of Advanced Technology, Kerman, Iran.

[6] School of Civil, Environmental and Architectural Engineering, Korea University, Seoul, Korea.

[7] Chief Research Engineer, Mechanical Engineering R&D Lab, LIG Nex1, Seung Nam, Korea.

[8] Division of Computational Mechanics, Ton Duc Thang University, Ho Chi Minh City, Vietnam.

[9] Faculty of Civil Engineering, Ton Duc Thang University, Ho Chi Minh City, Vietnam.

[*] Corresponding Author: Timon Rabczuk. Email: timon.rabczuk@tdtu.edu.vn.

Received: 29 April 2020; Accepted: 28 July 2020.

response and the obtained results may serve as valuable guide for future experimental and theoretical studies.

Keywords: Graphene, nanocomposites, bulletproofing, impact, PDMS.

1 Introduction

Synthesis and control of size and geometry of nanopores in materials are critical aspects for various applications, like in DNA sequencing [Izadifar, Abadi, Hossein Nezhad Shirazi et al. (2018)], ballistic protection materials to spread the impact of projectiles [Wu and Chang (1995); Zee and Hsieh (1998); Zhu, Goldsmith and Dharan (1992); Zhang, Sun, Chen et al. (2014)], particle therapy in cancer treatment [Jermann (2015)], and surface coating [Knotek, Bosserhoff and Schrey (1992)]. In some applications, the attempt is to determine the initial velocity and energy of the projectile to penetrate a target to make a hole or destroy it, and in some other cases, it is very important to control the hole's radius. Around 20 years after the idea of DNA sequencing was first proposed by Church et al. [Church, Deamer, Branton et al. (1998); Kasianowic, Brandin, Barton et al. (1996)] Oxford Nanopore Technologies offered a commercial nanopore sequencer in which protein nanopores is used to control the rate at which the DNA travels through the pores. To improve the performance of solid-state nanopore sensors, trigged scientists to make them thinner. In particular, graphene with atomic thick structure has recently gained remarkable application for DNA sequencing [Wasfi, Awwad and Ayesh (2018)]. Thereafter, many researchers investigated different experimental and numerical approaches to investigate how to drill nanopores in two dimensional materials like graphene by using electron beam [Schneider, Kowalczyk, Calado et al. (2010)] or through molecular dynamics (MD) simulations [Zhao, Xie, Liu et al. (2014); Berdiyorov, Mortazavi, Ahzi et al. (2016); Li, Liang and Zhao (2013)]. In medical applications like cancer treatment based on particle therapy, recognition of the initial velocity and energy of the projectile are substantial. In cancer treatment, particles like protons are used instead of X-ray in order to decrease the hazardous damages to the healthy tissue surrounding the target [Mohan and Grosshans (2016)]. Beams of protons with specific energy penetrate human tissues, reach the target and deliver maximum radiation dose near the tumor, minimizing damage to the surrounding normal tissues.

In some other applications, however, scientists try to develop new materials and composites that could reduce the penetration of the projectile into the target. In these cases, designers have no control over the velocity of the projectile, and therefore need to design a material that can minimize or prevents the hazardous effects of high velocity impact. Soldiers, police, and others who put themselves in harms conditions, needed bulletproof cloths that could protect their vital organs and could perform their jobs in relative safety. Kevlar and presumably other fabrics are used to spread the impact of caliber ammunition thus allow them to perform their jobs safely [Castaño and Rodríguez (2013)]. Experimental and analytical researches [Lee, Loya, Lou et al. (2014); Bizao, Machado, Sousa et al. (2018)] performed studies on the behavior of graphene sheet under extreme dynamic conditions. Lee et al. [Lee, Loya, Lou et al. (2014)] have found that the specific penetration energy for multilayer graphene is virtually 10 times more than the

literature values for macroscopic steel sheets at 600 meters per second. In their study, they realized combination of strength and toughness of material is needed to stop the speeding projectile as well as dissipating the absorbed kinetic energy.

Composite materials are currently considered as a reliable substitution to conventional materials for bulletproofing because of their improved characteristics such as light weight, high energy dissipation, and enhanced resistance against impact loadings. Graphene, the most prominent member of two dimensional materials presents ultrahigh tensile strength and stiffness. Moreover, polydimethylsiloxane (PDMS) is one of the most important elastomeric materials with high sticky feature and extensive application areas, ranging from medical, fabric, and interface material. In this work, we propose the graphene/PDMS composite structures for the bulletproofing application. We expect that due to the ultrahigh strength and stiffness of graphene, high viscous characteristic of PDMS, along with strong adhesion between graphene and PDMS, the resulting composite structures provide enhanced bulletproofing response. In order to examine the bulletproofing response of graphene/PDMS composite structures, for the first time we conducted extensive classical molecular dynamics simulations. In our modeling, we elaborately discuss the effects of different structural factors on the bulletproofing response.

The objective of this paper is to employ classical molecular dynamics simulations to systematically analyze how polymer base nanocomposites made of graphene resists high velocity projectiles. Worthy to note other methods like high order continuum mechanics theory can be employed to establish the results of bullet penetration in a media. Nonetheless for the considered problem in this work, molecular dynamics simulation is a more viable choice. Normally, the simulation of the penetration and rupture is challenging in the continuum modeling. Moreover, single or bi-layers graphene are in nanoscale that makes it difficult to model the adhesion section by a continuum mechanics approach. These effects are very difficult to be captured accurately in the continuum models, but are physically incorporated in the molecular dynamics simulations.

Recently, researches propose different fiber-reinforced polymer composites to enhance mechanical and electrical properties of materials that could not be found in conventional materials [Feng and Aymerich (2020); Wagih, Sebaey, Yudhanto et al. (2020); D'Aloia, Marra, Tamburrano et al. (2014); Zhang and Mi (2020); Abtew, Boussu, Bruniaux et al. (2019); Ji, Xu, Zhang et al. (2016); Parandoush and Lin (2017); Kakati and Chakraborty (2020)]. Most of the bulletproofing structures are made of strong synthetic fibers like kevlar [Jassal and Ghosh (2002)]. Kevlar is fabricated to strings or sheets which joined together by using adhesives like epoxy resins. The epoxy resins become brittle after curing, with poor resistance to crack initiation and growth [Unnikrishnan and Thachil (2012)]. Although Kevlar improves the resistance against the penetration of bullet, presence of brittle compound like epoxy resin causes failure at the resin between piles when the compression in the top layer and tension in the bottom layer happens due to the projectile impact and also the hardness of resin creates bruising in sensitive organs. In addition, quickly absorb of moisture and very poor resistance to UV makes Kevlar very sensitive to the environment [Yahaya, Sapuan, Jawaid et al. (2016); Connor and Chadwick (1996)]. Therefore, due to these disadvantages and on the side ultrahigh tensile strength and stiffness of graphene, researcher's attention have moved towards using this

novel material to be employed in bullet resistant structures with high strength to weight ratio [Lee, Loya, Lou et al. (2014); Girish, Tushar and Shreenidhi (2019); Njoroge (2013)]. To practically use graphene sheets, they are embedded in the polymers to fill the disconnectivities between separate graphene nano membranes. Worthy to remind that polydimethylsiloxane (PDMS) with high versatile applications [Ammar, Ramesh, Vengadaesvaran et al. (2016); Wang, Zhao and He (2016); Li, Zhao, Hu et al. (2012); Edouk, Faye and Szpunar (2017)] can be used to create lightweight and flexible graphene nanocomposites [Chen, Xu and Ma (2013)], which can be used against bullet damages.

2 Modeling

MD simulations are carried out by using large-scale atomic/molecular massively parallel simulator (LAMMPS) [Plimpton (1995)], and the atomic results are visualized by OVITO [Stukowski (2009)] package. Different models are subjected to a high velocity projectile, and then the results are analyzed and compared. These different models are as follows: single- and bi-layers graphene sheets, graphene/PDMS composite with different thicknesses and dimensions, and finally pure PDMS. In the case of graphene/PDMS composite, single- and bi-layers graphene are located on top or in between PDMS models. The process is as follow: First, the modified Markov scheme [Allen and Tildesley (1987)] is used to construct the amorphous PDMS with the density of 0.92 g/cc. Then the constructed model is introduced in LAMMPS for further analysis. After the relaxation the model is compressed in x-direction in order to obtain PDMSs with different thicknesses and dimensions. Then the constructions with different thicknesses and dimensions are replicated in x-direction with a gap between replicated models. In this case the size of the gap depends on the number of graphene layers which are supposed to be located on top of the model or in between. Afterwards, graphene layers and the bullet are constructed by developing python programming language code and then they are introduced to each model and whole the structure is introduced in LAMMPS. All the edges are fixed and different initial velocities are applied to bullet as an impact load to different models and the obtained results are discussed and compared. In the case of analysis of the one and 2-layers pure graphene, the planar size of graphene sheets was assumed to be 114.5 and 124.5 Å in y and z-directions, respectively. The diamond projectile with a diameter of 20 Å was made from 207 carbon atoms in all cases. In case of only graphene the distance between graphene layers for bi-layers graphene was considered to be 3.4 Å. An initial gap of 3.8 Å between projectile and graphene layers exists. The projectile moves along negative x-direction as a rigid object to avoid disintegration during the impact. All the graphene edges were fully clamped and AIREBO force field is utilized to describe all the intra and inter-molecular interactions, and 0.1 fs time step is considered. The AIREBO potential is used for a system of carbon and/or hydrogen atoms. The formula for this potential consists of three terms: The first potential called EREBO that has the same functional form as the hydrocarbon REBO potential developed in Brenner et al. [Brenner, Shenderova, Harrison et al. (2002)]. The coefficients for EREBO essentially the same as coefficients are used in Brenner et al. [Brenner, Shenderova, Harrison et al. (2002)]. The second potential is ELJ that adds longer-ranged interactions using a form similar to Lennard-Jones potential [Plimpton (1995)]. The third potential is called ETORSiON which is an explicit four-body potential that describes various dihedral angle preferences in hydrocarbon configurations [Plimpton (1995)]. The

complete and detailed formula for AIREBO force field are given in [Stuart, Tutein and Harrison (2000)]. In the case of graphene/PDMS composite or pure PDMS, a small time step of 0.25 fs is used due to the existence of fast vibration of hydrogen atoms. The condensed-phase optimized molecular potentials for atomistic simulation studies (COMPASS) potential was used, which has been optimized for PDMS by fitting to ab initio calculations [Sun (1998); Sun and Rigby (1997); Sun (1995)]. COMPASS force field, like the others force field, has two parts: The formulas that define it and the coefficients used for a particular system. In COMPASS force filed there are collection of formulas [Plimpto (1995)] that describe the time evolution of bond length, bond angels and torsions, and also non-bonding Van der Waals and electrostatic interaction between atoms. For the PDMS, COMPASS force field coefficients are completely stablished by Sun et al. [Sun (1998); Sun and Rigby (1997); Sun (1995)]. In the composite form of PDMS and graphene, also, hybrid pair style introduced to enable the use of multiple pair styles in the simulation and the assignment of pair styles to type pairs is made via the pair_coeff command in LAMMPS [Plimpton (1995)].

3 Results and discussions

3.1 Pure graphene

The impact simulation is conducted with NVE (micro-canonical) ensemble. The projectile starts to move toward the graphene as shown in Fig. 1, and the time history for the projectile's displacement and its kinetic energy for one layer graphene are plotted in Fig. 2. Before the contact, projectile moves through the gap, the kinetic energy remains constant. As the impact happens, the kinetic energy starts to decrease. Depending on the bullet's initial velocities, 3 different cases happen: Case (1), the projectile's initial velocities are lower than 5200 m/s and there is no enough kinetic energy to breaks bonds of the graphene layer. The projectile hits the graphene, pushes the graphene and reaches maximum displacement, stops for an instant that at this time it has zero kinetic energy. The stretched graphene causes the bullet bounces back with lower kinetic energy than its initial kinetic energy. Figs. 2(a) and 2(b) show this case. Case (2), as is shown in Figs. 2(c) and 2(d), the projectile's initial velocities are between 5500 m/s and 10000 m/s. In these range of speeds, the projectile starts to break some graphene's bonds but the complete perforation does not happen. After breaking some bonds, the projectile sticks to graphene layer and all system vibrates together. Case (3), as represented by Figs. 2(e) and 2(f), the projectile's initial velocities are more than 10500 m/s. In this case the projectile completely passes through the graphene layer and complete perforation happens. The projectile loses some of its kinetic energy, passes through the graphene, and with constant kinetic energy continues to move in the negative x-direction. In the case of 2-L graphene similar scenario happens, however, with different higher initial velocities compare to one layer. For the 2-L graphene for velocities up to 6000 m/s the bullet bounces back, however, initial velocities more than 16000 m/s the complete perforation could happen. For the velocities between 6000 m/s and 16000 m/s some bonds break and the bullet sticks to graphene layers and whole the system vibrates.

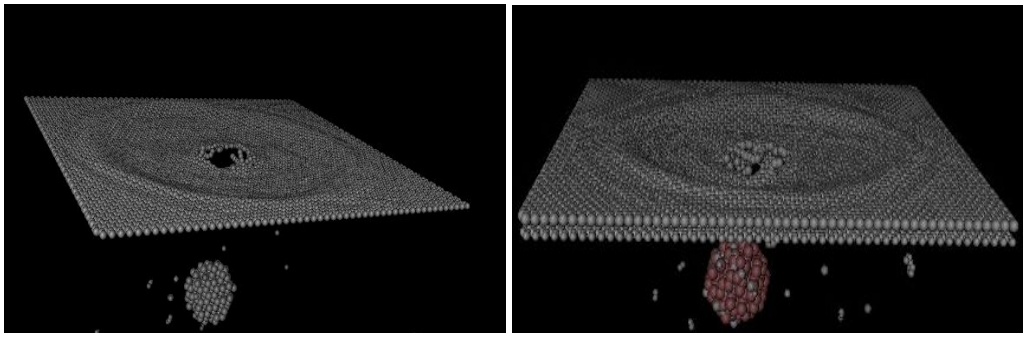

Figure 1: One and 2-L graphene subjected to high velocity projectile and complete perforation happens

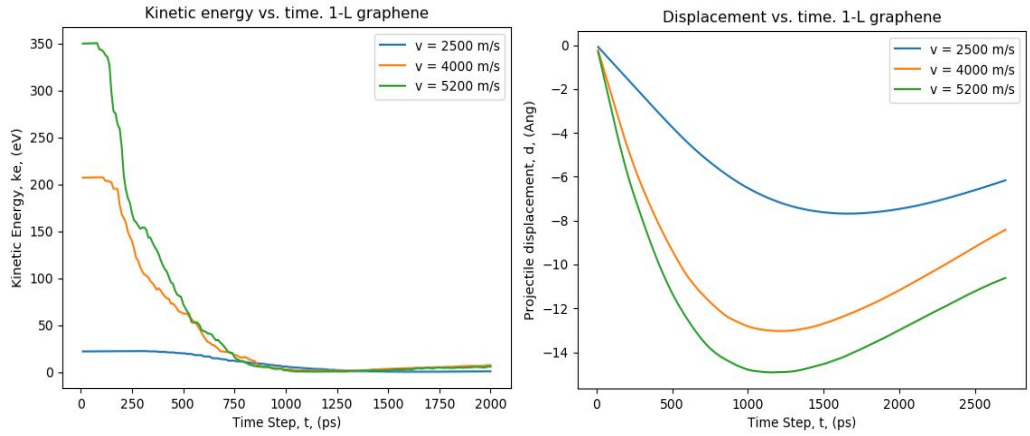

(a) (b)

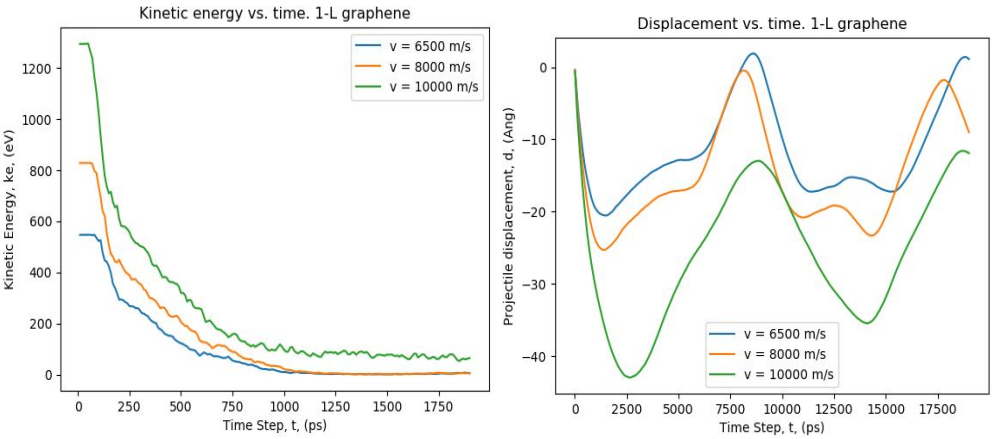

(c) (d)

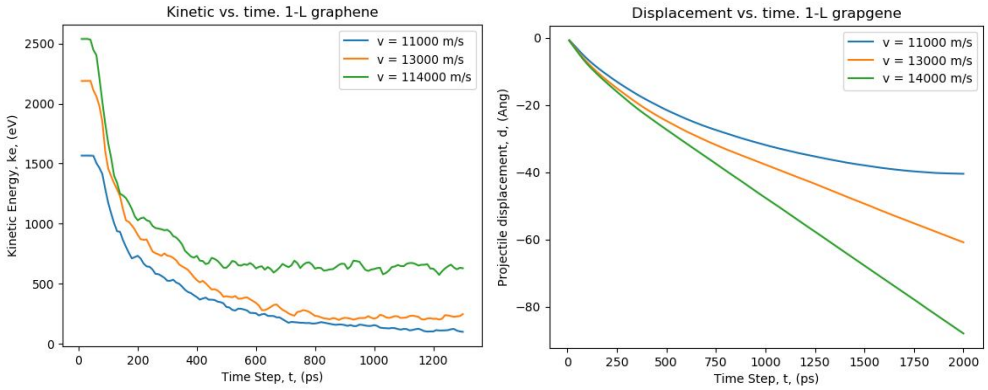

(e) (f)

Figure 2: Projectile's time history when impacts one layer graphene. Change of kinetic energy versus time and displacement time history for different projectile's initial velocities are plotted

It should be mentioned that our predicted velocities are relatively high compared to those numerical results in Gama et al. [Gama, Chowdhury and Gillespie Jr (2016)] in which complete perforation happens from 4500 to 8000 m/s for single- and bi-layer graphene. In the study by Gama et al. [Gama, Chowdhury and Gillespie Jr (2016)] mass of the projectile consists of 180 which is lower than the present study in which projectile's mass consists of 207 carbon atoms. This should result in that in present study perforation has to happen in lower velocities than those obtained by Gama et al. [Gama, Chowdhury and Gillespie Jr (2016)]. However, as the projectile's diameter was 12 Å in the study by Gama et al. [Gama, Chowdhury and Gillespie Jr (2016)], which is nearly two times lower than the projectile's diameter of 20 Å, in the present study. As the projectile diameter increases, the contact surface increases, therefore more initial velocity is needed for the complete perforation. This is the reason why in the present study perforation happens in such velocities so higher than the velocities in Gama et al. [Gama, Chowdhury and Gillespie Jr (2016)].

In order to conduct a numerical validation, a model similar to that was conducted by Gama et al. [Gama, Chowdhury and Gillespie Jr (2016)], (single-layer graphene with the dimensions of 200×200 Å and a projectile with a radius of 12 Å) is constructed. The complete perforation happens for the initial velocities higher than 5000 m/s, which is in a close agreement with the results in the work by Gama et al. [Gama, Chowdhury and Gillespie Jr (2016)], that suggests the perforation happens for the initial velocities higher than 4500 m/s. Also a model constructed similar to that experimented by Lee et al. [Lee, Loya, Lou et al. (2014)], (projectile with the mass $m=3.61\times10^{-24}$ kg) and complete perforation happened at the minimum velocity equal to 630 m/s which is in a good agreement by 600 m/s obtained by Lee et al. [Lee, Loya, Lou et al. (2014)].

Worthy to note that the velocity of conventional bullets is in the range of 1000-2000 m/s. In our theoretical analysis, we found the velocities that the projectile's impact can result in the rupture of the graphene. Nonetheless, if we have used larger diameters for the diamond particle, the mass would increase and the rupture would occur at lower

velocities. This way, our results like other theoretical simulations can be useful to comparatively study the composite designs, rather than concentrating on the absolute values of the projectile's velocity.

3.2 PDMS and graphene nanocomposites

A bulk PDMS was constructed with a dimension of 79.1×54.13×57.97 Å in x, y, and z directions respectively. Then the construction compressed in the x-direction and 3 models with different dimensions are obtained: 16×94.94×102.34 Å, 21×87.5×90.63 Å and 26×78.3×87.52 Å which here are called as model 1, 2, and model 3 respectively. Then these three models are replicated in the x-direction and one and 2-L graphene sheets, which are introduced in between and surface of each model. Distances between graphene layers, and graphene and PDMS were considered 3.4 Å, and the distance between PDMS bulks during replication is considered 4.5 Å. The diameter of the diamond bullet was the same as before, 20 Å. The graphical views of different models for each case are shown in Fig. 3. In Fig. 3, Figs. 3(a), 3(b) and 3(c) represent one layer graphene is located on top of models 1, 2 and 3, respectively. Figs. 3(d)-3(f) show 2-L graphene are located on top of models 1, 2 and 3, respectively. Figs. 3(g)-3(i) express one layer graphene is located in between of Models 1, 2 and 3, respectively. And finally, Figs. 3(j)-3(l) represent 2-L graphene are located in between of model 1, 2 and 3, respectively. All models are completely clamped at edges and are exposed to the diamond bullet which remains rigid through all simulation time and impacts the targets at the center. In all simulations time step is considered as 0.25 fs. The impact simulation is conducted with NVE (micro-canonical) ensemble. First we try to observe minimum velocity that results in the first bond of graphene on top and in between for each model breaks and the results are tabulated in Tab. 1 and the graphical pictures are shown in Fig. 4 for two sample models to demonstrate what here means by breaking the first bond. The first breaking bonds are shown by arrows. In these three models it could be seen that when one layer graphene is located on the top, the first bond-breaking happens virtually at the same impact velocities. For one layer on top, the breaking happens at 6200 m/s, 6200 m/s, and 6100 m/s for Models 1, 2, and 3 respectively. This means the thickness of the PDMS on the behind of the graphene does not contribute to strengthening the graphene. For 2-L graphene on top, the first bond breaks in lower velocities compare to one layer and the reason for this is that as the number of layers increases, in fact moving from nano-scale to micro- scale, the material properties such as elasticity modulus and breaking strength decrease and as a result the first bond breaks in lower energy. However, if just consider the 2-L graphene on top, the first bond breaks nearly at the same velocities, 5500, 4500, 5000 m/s for Model 1, 2, and 3 respectively that similarly again states that the Thickness of the PDMS behind of the graphene layers does not contribute significantly to improve composite impact loading.

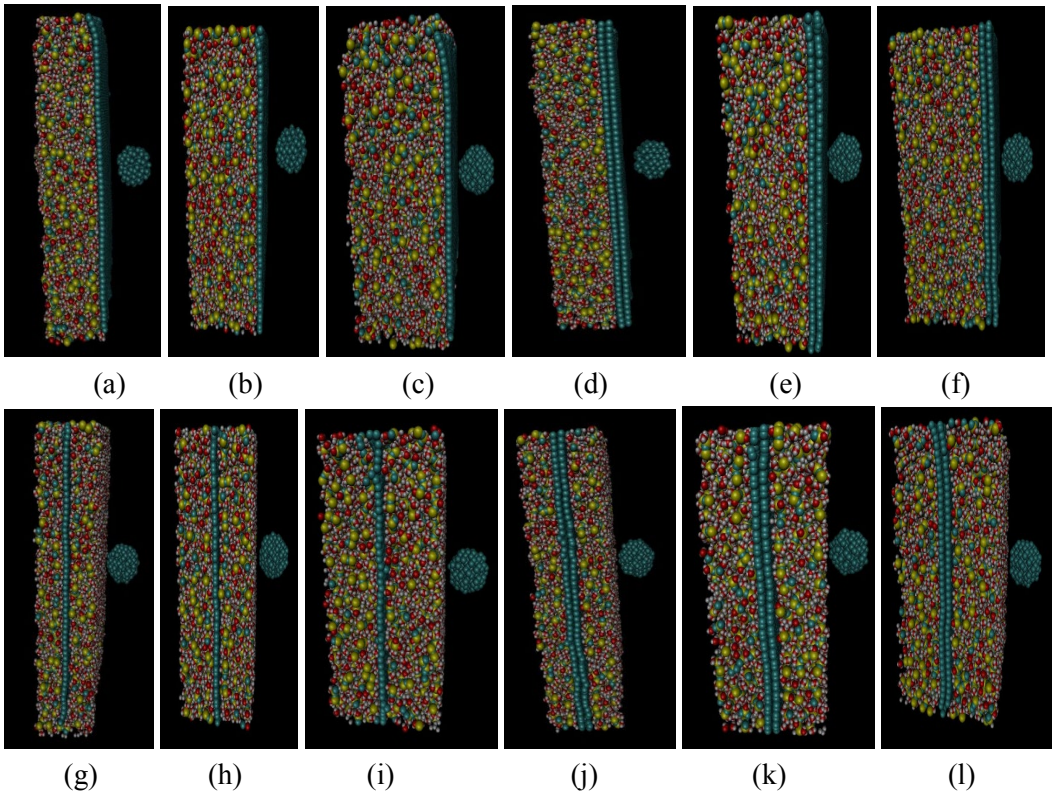

Figure 3: Different molecular models considered in this work. One and 2-L graphens are located on top or between for different PDMS models

Table 1: The minimum projectile's velocity that could breaks a first bond. Here B and T stand for the location of graphene in between and top, respectively

Model	Model I				Model II				Model III			
Graphene location	1-T	1-B	2-T	2-B	1-T	1-B	2-T	2-B	1-T	1-B	2-T	2-B
Perforation velocity (m/s)	6200	12500	5500	16500	6200	17000	4500	17500	6100	19500	5000	22500

The scenario is completely different when the graphene layers are located in between the PDMS. When one layer graphene is located in between, the first bond breaks at initial velocities, 12500, 16500, and 19500 m/s for Models 1, 2 and 3 respectively which these velocities are not only considerably higher than the case of one layer graphene located on the top, but also they increase significantly from Models 1 to 3 in which the thickness of the PDMS increases. In the case of graphene layers in between, at first, projectile enters the PDMS, unlike the case of graphene layers on top that the projectile at first impacts the graphene. When the Projectile enters the PDMS, a resistance force applies to the

projectile due to the stickiness of the PDMS. This resistance force decreases the velocity of the projectile before reach to the graphene and this resistance force increases with the thickness of the PDMS. Therefore, in the case of graphene layers in between, more initial velocity is needed to break the first bond compare to the case in which graphene layer located on top. Also, the higher PDMS thickness, the projectile needs higher initial velocity to pass through the PDMS and impacts the graphene and because of that the initial velocity increases from Model 1 to Model 3. In the case of 2-L graphene located in between, the first bond breaks at initial velocities, 16500, 19500, and 22500 m/s for Models 1, 2, and 3 respectively. These initial velocities increase from Model 1 to Model 3 because of the PDMS thickness increases. However, compare to layers on top, in which the first bond of 2-L graphene breaks easily than one layer on top, where it can be seen that 2-L graphene in between needs higher initial velocity to break the first bond compare to one layer in between and this seems the 2-L in between causes the PDMS be more coherent than one layer. In fact as the number of graphene layers in between increases, the PDMS seems more coherent and as a result stickier.

Table 2: The minimum projectile's velocity could make dynamical perforation for each model. Here B and T stand for the location of graphene in between and top, respectively

Model	Model I				Model II				Model III			
Graphene location	1-T	1-B	2-T	2-B	1-T	1-B	2-T	2-B	1-T	1-B	2-T	2-B
Perforation velocity (m/s)	10300	18500	14500	26000	10400	24500	14000	34500	10500	28000	15000	40000

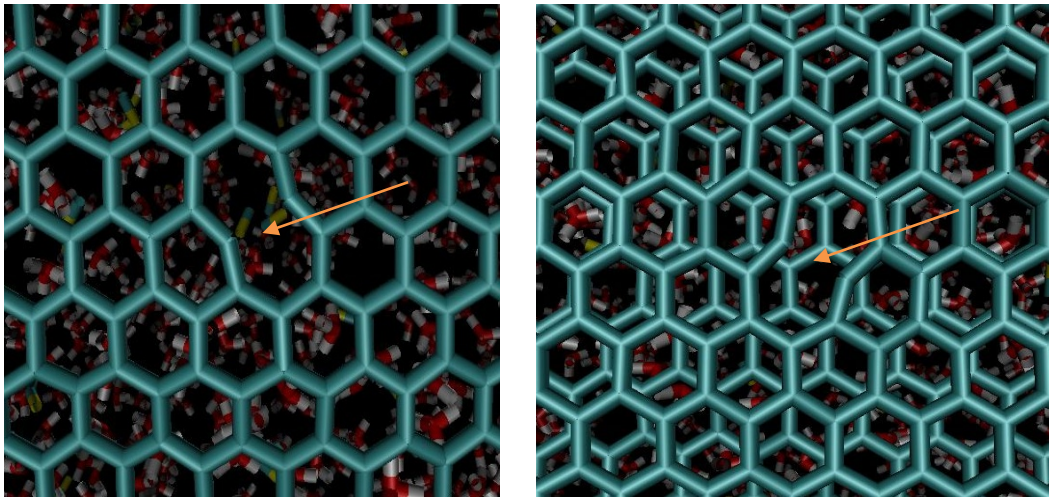

(a) (b)

Figure 4: The minimum velocity that breaks the first bond in PDMS-graphene composite. (a): One graphene layer settled on top of the PDMS, model 1. (b): 2-L graphene located on top of the PDMS, model 2

In all models and each case that the initial velocities are higher than the minimum velocities in which first bond breaks, two different outlines happen. If the initial velocities are high enough to pass through the whole composite, called complete perforation happens. The minimum complete perforation velocities for all models and all cases are listed in Tab. 2 and graphical views are depicted in Fig. 5 for some typical cases and models to demonstrate the complete perforation. For the velocities between minimum velocities that first bond breaks, velocities in Tab. 1, and minimum velocities that complete perforation happens, velocities in Tab. 2, the projectile impact graphene layers, break more than one bond but does not pass through the whole composite. The number of broken bonds strongly depends on the initial velocity.

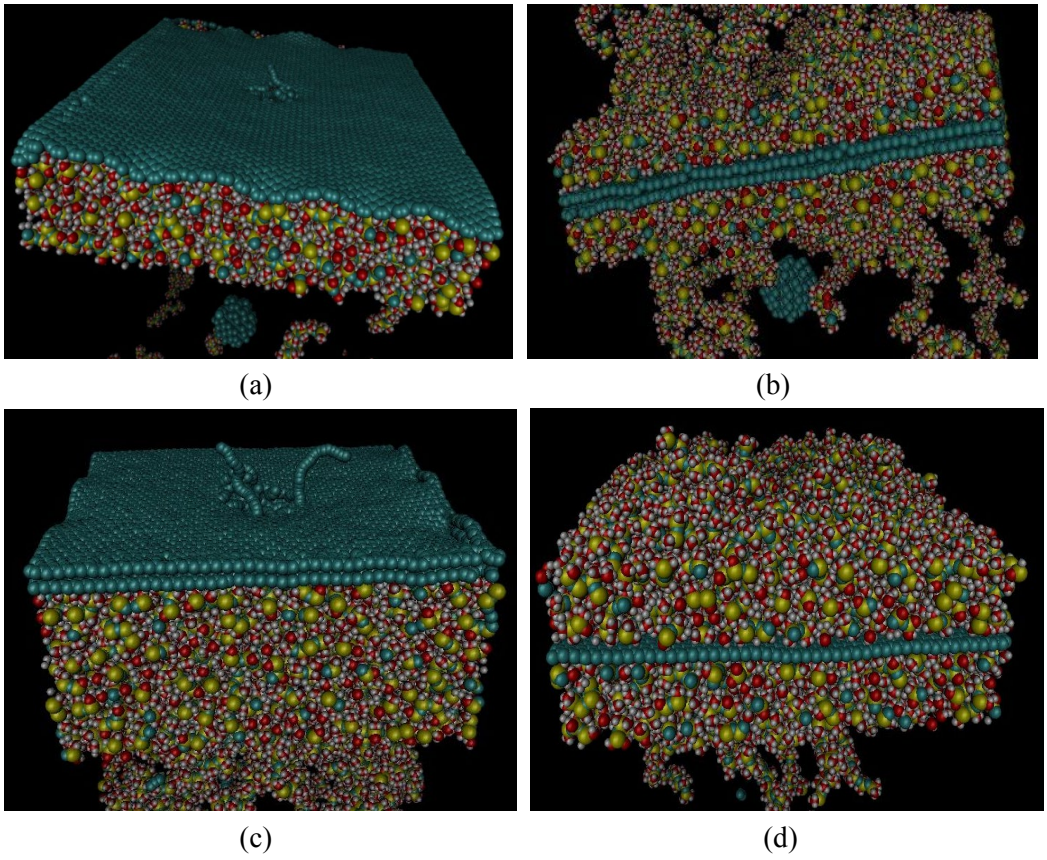

Figure 5: Perforation in different models. (a): One graphene layer on top of the PDMS in Model 1. (b): 2-L graphene embedded in between PDMS in Model 1. (c): 2-L graphene on top of the PDMS in Model 3. (d): One graphene layer embedded in between PDMS in Model 2

Now we try to follow the bullet's excursion and change of its kinetic energy and displacement versus time. In the manifestation of graphene layers on the top three different cases happen: Case (1), the bullet moves with an initial velocity, but not enough to breaks any bonds. In this case, the bullet moves with constant velocity or kinetic energy to pass

through the gap between bullet and graphene layers, then impacts graphene layers and pushes it in negative x-direction, reaches the maximum displacement and transfers all of its kinetic energy as potential energy to the composite or here is called target, graphene and PDMS. Then some potential energy of the target transferees to the bullet as kinetic energy and causes the bullet bounces back and continues to move along positive x-direction with constant kinetic energy. The amount of converted potential energy to kinetic energy is very low compare to the initial kinetic energy of the bullet. Case (2): the initial kinetic energy of the system is higher than Case (1), but not enough to create complete perforation. The bullet hits the target, pushes the target and breaks some bonds of the graphene layers, and then bounces back similar to Case (1). Case (3), bullet's initial kinetic energy is big enough to create complete perforation in graphene layers and enters the PDMS. Depending on the initial kinetic energy and the thickness of the PDMS, the bullets may trap inside the PDMS or passes through it. Whether the bullets trap inside the PDMS or pass through, depends on the thickness of the PDMS as well as the velocity that bullet enters the PDMS after complete perforation in graphene layers. The movement of the projectile inside the PDMS will be discussed in more detail in section IV. To plot the time history, we consider Tabs. 1 and 2, to select the initial velocity of the projectile for each case and different models. As an example, to demonstrate time history in Case (1), for one layer graphene located on top of the model one, three initial velocities are considered, 3000, 4500, and 6000 m/s, which all are lower than the velocity, 6200 m/s, that projectile is able to break the first bond in this case. The results for the graphene layer located on top are plotted in Fig. 6. As we discussed before, all graphs in Fig. 6 show the kinetic energy is constant while the projectile passes through the initial gap between the projectile and the target. The kinetic energy decreases sharply until it becomes zero, and then increases slightly but not considerably. Finally, the projectile continues to moves with constant kinetic energy. The displacement time history shows, in this case for all models, The projectile starts to move in the negative x-direction, reaches the maximum displacement, and then bounces back, continuous to move in opposite x-direction.

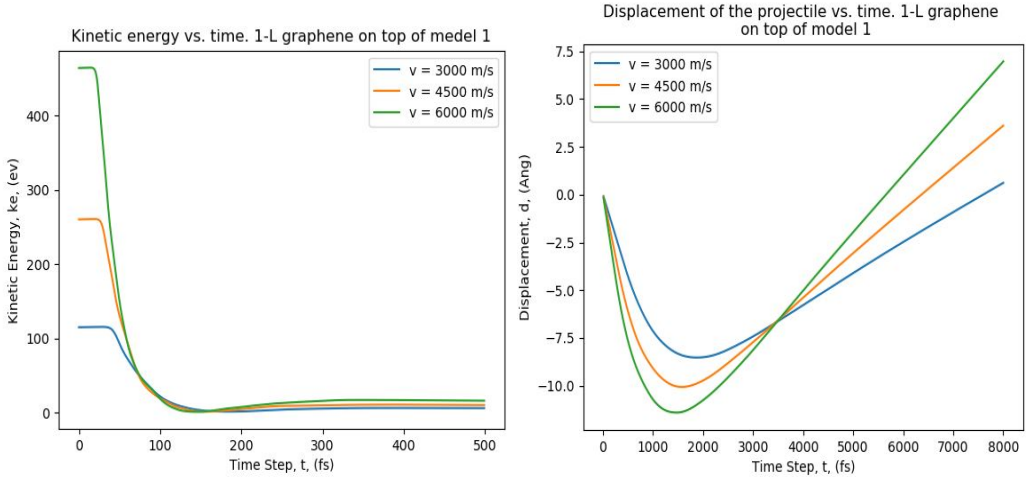

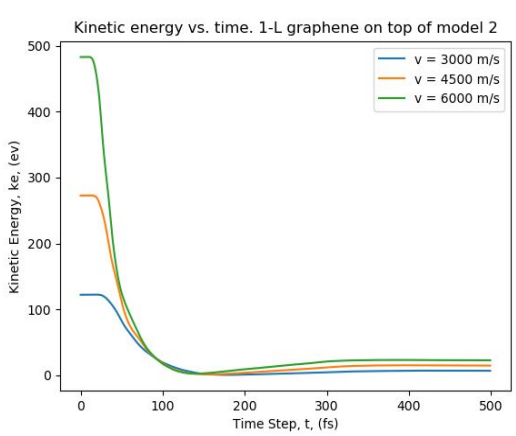
Kinetic energy vs. time. 1-L graphene on top of model 2
v = 3000 m/s
v = 4500 m/s
v = 6000 m/s
Kinetic Energy, ke, (ev)
Time Step, t, (fs)

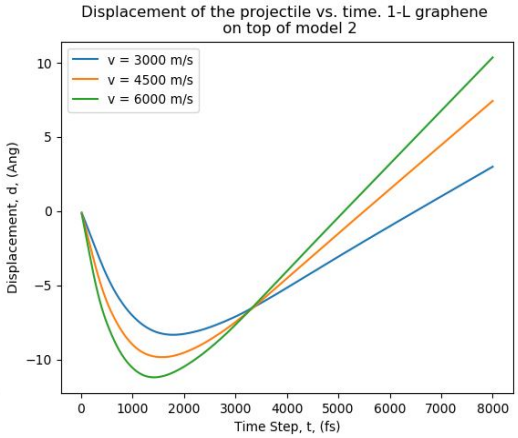
Displacement of the projectile vs. time. 1-L graphene on top of model 2
v = 3000 m/s
v = 4500 m/s
v = 6000 m/s
Displacement, d, (Ang)
Time Step, t, (fs)

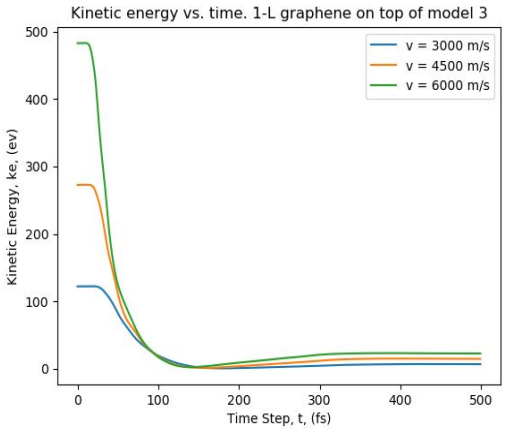
Kinetic energy vs. time. 1-L graphene on top of model 3
v = 3000 m/s
v = 4500 m/s
v = 6000 m/s
Kinetic Energy, ke, (ev)
Time Step, t, (fs)

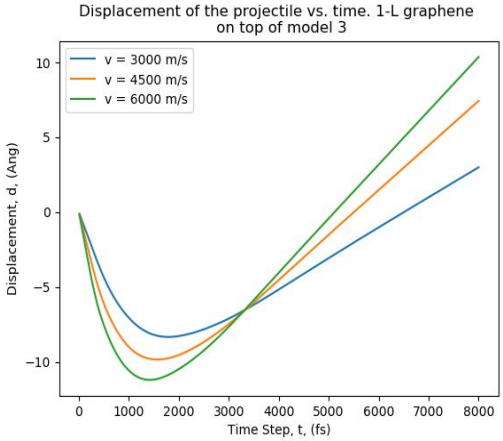
Displacement of the projectile vs. time. 1-L graphene on top of model 3
v = 3000 m/s
v = 4500 m/s
v = 6000 m/s
Displacement, d, (Ang)
Time Step, t, (fs)

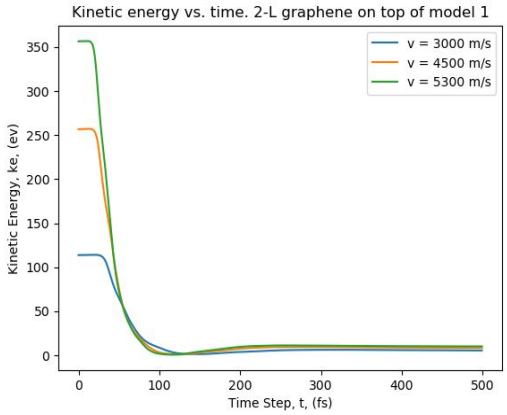
Kinetic energy vs. time. 2-L graphene on top of model 1
v = 3000 m/s
v = 4500 m/s
v = 5300 m/s
Kinetic Energy, ke, (ev)
Time Step, t, (fs)

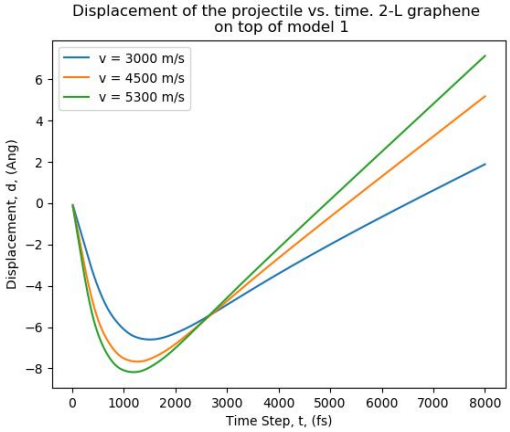
Displacement of the projectile vs. time. 2-L graphene on top of model 1
v = 3000 m/s
v = 4500 m/s
v = 5300 m/s
Displacement, d, (Ang)
Time Step, t, (fs)

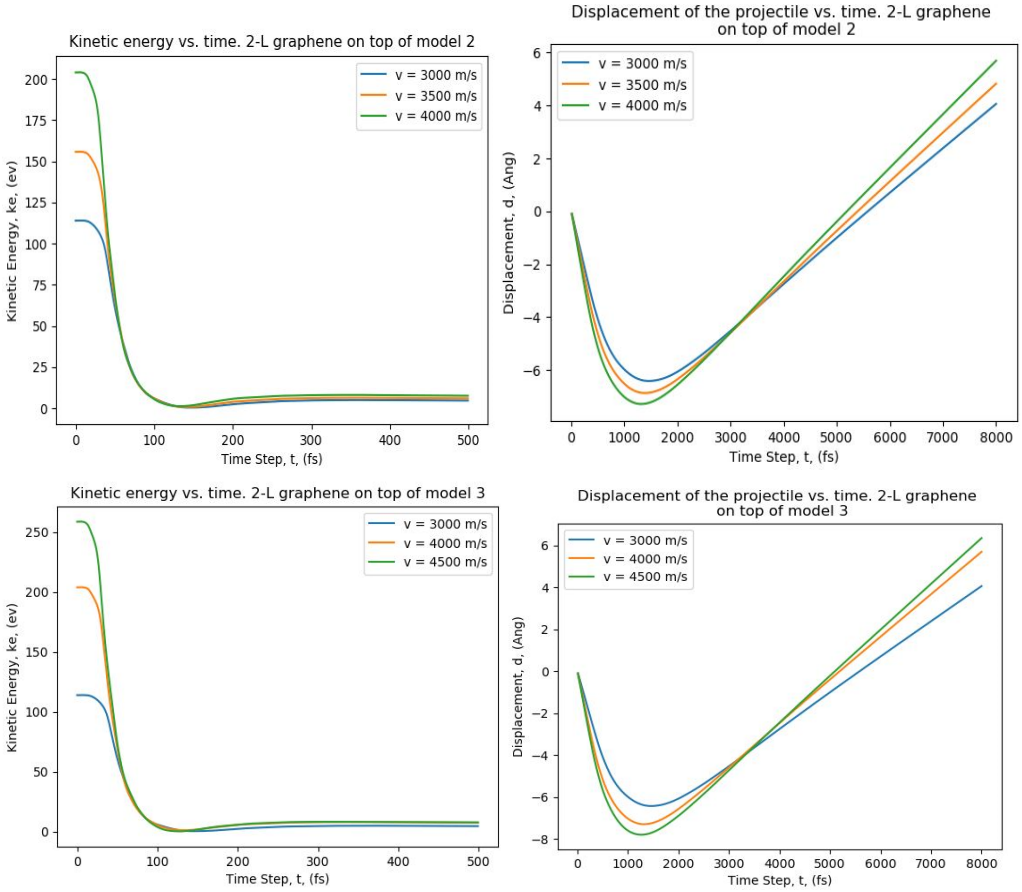

Figure 6: Projectile's kinetic energy and displacement time history for one and 2-L graphene are located on top of Models 1, 2 and 3

It can be seen that for all models the thickness of the PDMS does not affect the maximum displacement of the projectile, but the number of the graphene layers does. For example, for one layer graphene over PDMS surface, just the thickness of PDMS changes, for the equal initial velocity of 3000 m/s the maximum displacements are around 7.5 Å, however, for the same velocity for the case 2-L graphene on top in all models the maximum displacements are around 6.0 Å. This means as long as the graphene layers are located on the top, PDMS does not contribute significantly to improve the composite characteristics, however, the number of graphene layers does. The manifestation of graphene layers located in between, the scenario is different. As the bullet moves toward the composite, at first it contacts the PDMS. Depends on its initial velocity, it could have the opportunity to reach the graphene or not. The movement of the projectile in PDMS will be discussed in section IV. Similar to the graphene layers on top, depends on the initial velocity of the projectile, three different cases happen, but in detail not exactly same as what happens in graphene layers on top: The bullet trapped inside the PDMS and does not reach to the graphene or impact graphene and bounces back without any bond

breaking in graphene, called Case (1). When the bullet bounces back, depend on the initial velocity and the PDMS thickness, maybe it could completely exit the PDMS or tarps inside the PDMS on its way back. This case, Case (1), happens when all initial velocities are smaller than the velocities that could break the first bond. Case (2), bullet impacts graphene breaks some bonds and bounces back again. Similar to the Case (1), on its way back maybe completely be able to exit PDMS or traps inside the PDMS, depend on the PDMS thickness and initial velocity of the projectile. Case (3), the bullet impacts graphene, makes complete perforation in graphene and enters the PDMS behind the graphene. The projectile time histories for graphene layers are located in between for Case (1) in all models are plotted in Fig. 7.

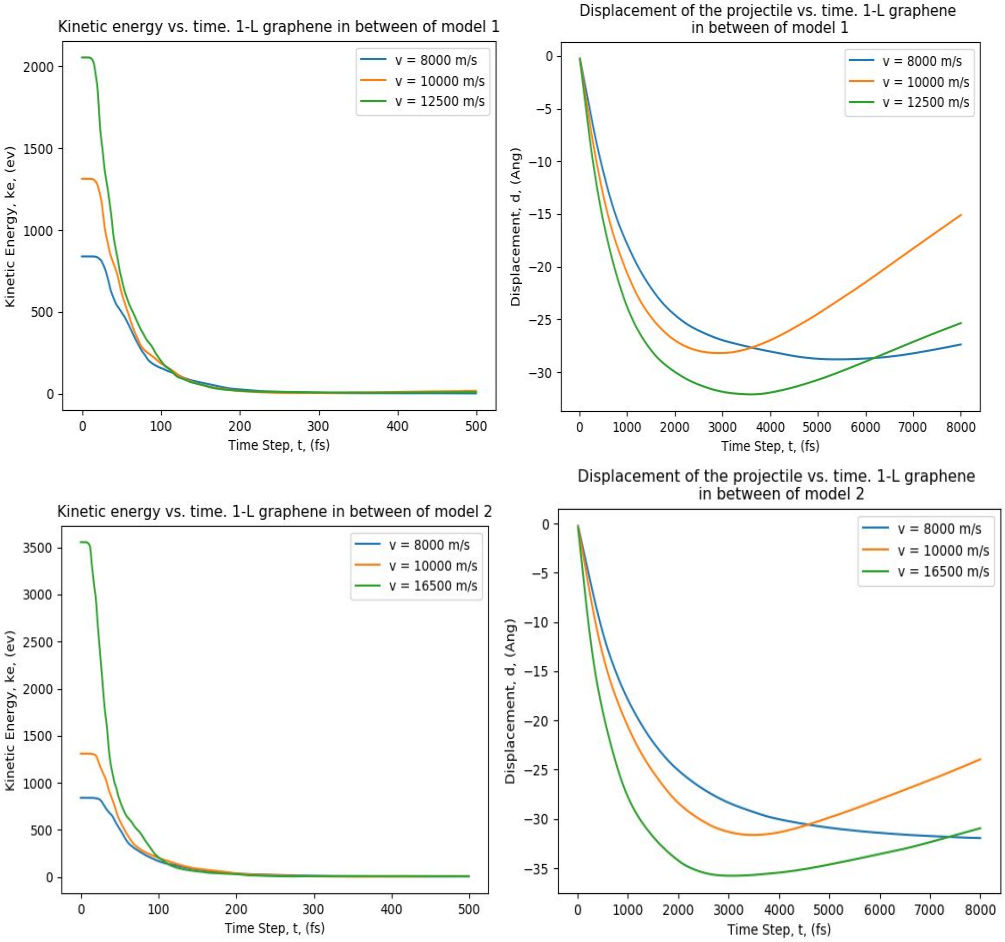

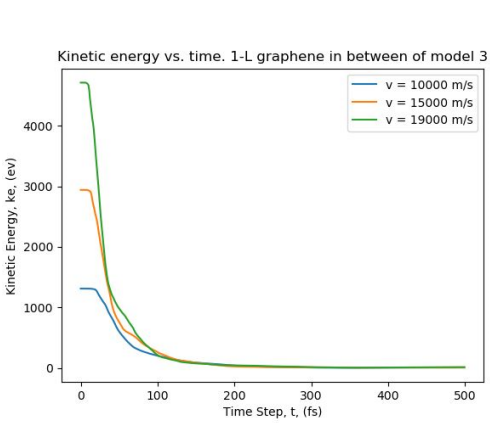
Kinetic energy vs. time. 1-L graphene in between of model 3
v = 10000 m/s
v = 15000 m/s
v = 19000 m/s
Kinetic Energy, ke, (ev)
Time Step, t, (fs)

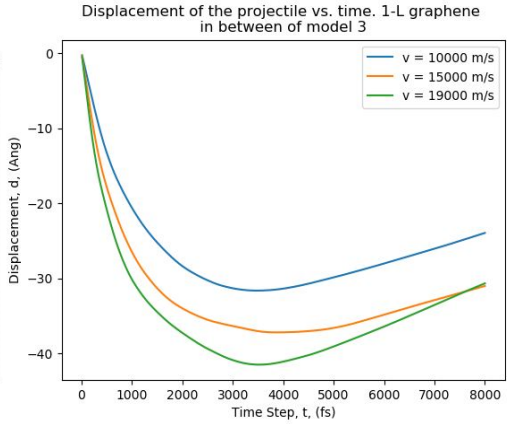
Displacement of the projectile vs. time. 1-L graphene in between of model 3
v = 10000 m/s
v = 15000 m/s
v = 19000 m/s
Displacement, d, (Ang)
Time Step, t, (fs)

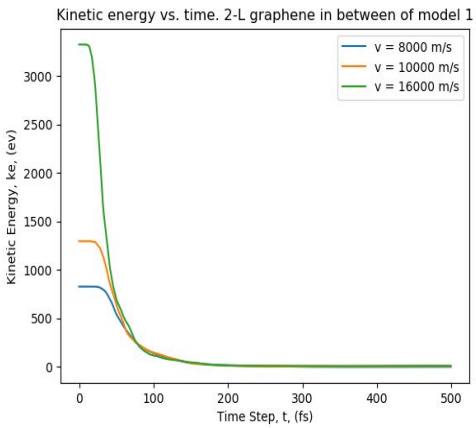
Kinetic energy vs. time. 2-L graphene in between of model 1
v = 8000 m/s
v = 10000 m/s
v = 16000 m/s
Kinetic Energy, ke, (ev)
Time Step, t, (fs)

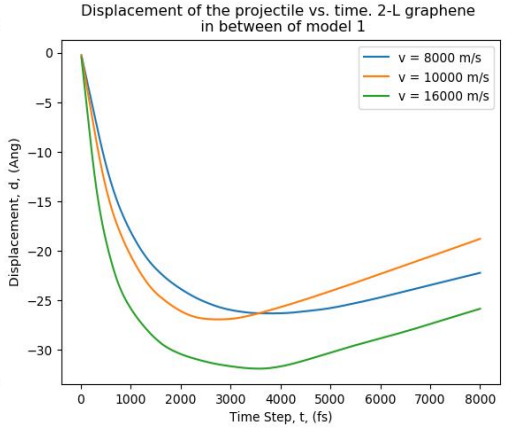
Displacement of the projectile vs. time. 2-L graphene in between of model 1
v = 8000 m/s
v = 10000 m/s
v = 16000 m/s
Displacement, d, (Ang)
Time Step, t, (fs)

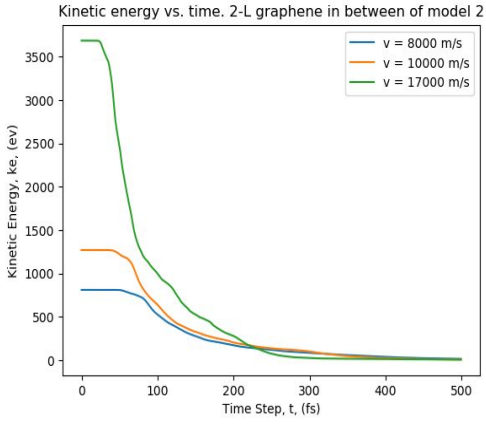
Kinetic energy vs. time. 2-L graphene in between of model 2
v = 8000 m/s
v = 10000 m/s
v = 17000 m/s
Kinetic Energy, ke, (ev)
Time Step, t, (fs)

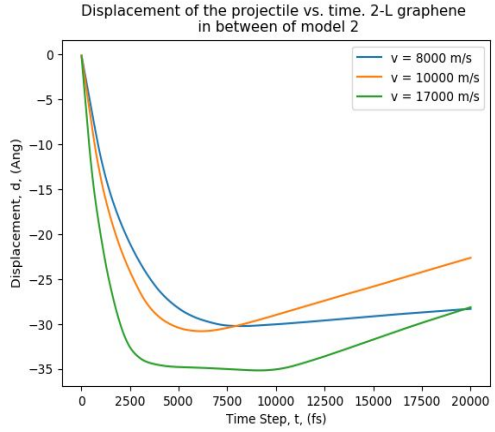
Displacement of the projectile vs. time. 2-L graphene in between of model 2
v = 8000 m/s
v = 10000 m/s
v = 17000 m/s
Displacement, d, (Ang)
Time Step, t, (fs)

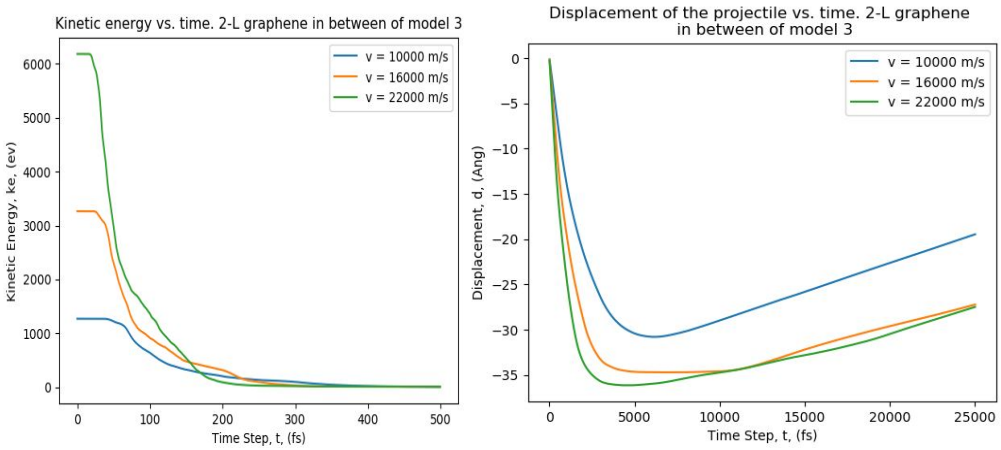

Figure 7: Projectile's kinetic energy and displacement time history for one and 2-L graphene are located in between for Models 1, 2 and 3

As it could be seen, Fig. 7 reveals that at some velocities the bullet could not impact the graphene layers and trapped inside the PDMS, as stated before. For example for Model 2 in the case one graphene layer in between, the initial velocity equal to 8000 m/s is not big enough to provide contact between bullet and graphene. It can be seen the bullet approximately stops and there is not a big change in displacement as time goes on and its kinetic energy approaches to zero. Also, in some initial velocities the projectile may impact the graphene, but trap inside the PDMS when it bounces back, as an example one and 2-L graphene in between of Model 1 and Model 2 respectively, where the velocities are 8000 m/s. For the Case (2) in which the projectile breaks some bonds and bounces back and Case (3) that the projectile creates complete perforation, the graphs are included in supporting information document, Figs. S1-S4 for all models. In a case which complete perforation happens, Case (3), for all models it could be seen that as the perforation in graphene happens, the steep of projectile displacement is constant, means after complete perforation of graphene projectile moves with a constant velocity, no matter the graphene layers are located on top or in between. That seems when the projectile impacts graphene makes the PDMS behind it disintegrated as if the PDMS behind the graphene exploded. It means PDMS behind the graphene does not contribute to improving the composite features exposed to the bullet, however, if the bullet first enters the PDMS, the PDMS forward the graphene, the composite features improve enormously. A graphical view of PDMS disintegration when it is located behind the graphene layers are shown in Fig. S5. From the above discussion it could be concluded that introducing two extra layers graphene at the end of each model prevents the dissociation of PDMS behind the graphene which results in a composite with high resistance to the high-velocity projectiles.

3.3 Thick PDMS

In the former section it was seen that the thickness of the PDMS and number of graphene layers improve bullet resistance of the graphene-polydimethylsiloxane composite. This

improvement is significant when graphene layers are embedded inside the PDMS rather than located on the top and that triggers off to trace the movement of the projectile inside the PDMS more in-depth. In most of the polymers their backbone is primarily carbon-based, and they are called organic polymers. However, some polymers have inorganic backbones and PDMS is one of those that its backbone constitutes of alternating silicon (Si) and oxygen (O). Silicon like carbon has four free electrons and could form four chemical bonds. In PDMS's monomer, silicon is bonded to oxygen and two methyl groups (Fig. 8). It is a highly applicable material in conditions like sealing application, medical plants, lubricating, and so on. When it could not be cross-linked, it is a highly viscous liquid. When it is cross-linked is called silicon rubber or just silicon. Generally, PDMS has a glass transition below than room temperature (Tg<25) and as it has elastomeric features, it could be used at room temperature. In this paper the model is not considered cross-linked, however, it has a very high viscosity and could remain virtually solid in ambient conditions.

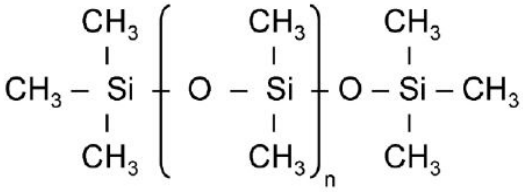

Figure 8: Polydimethylsiloxane chemistry

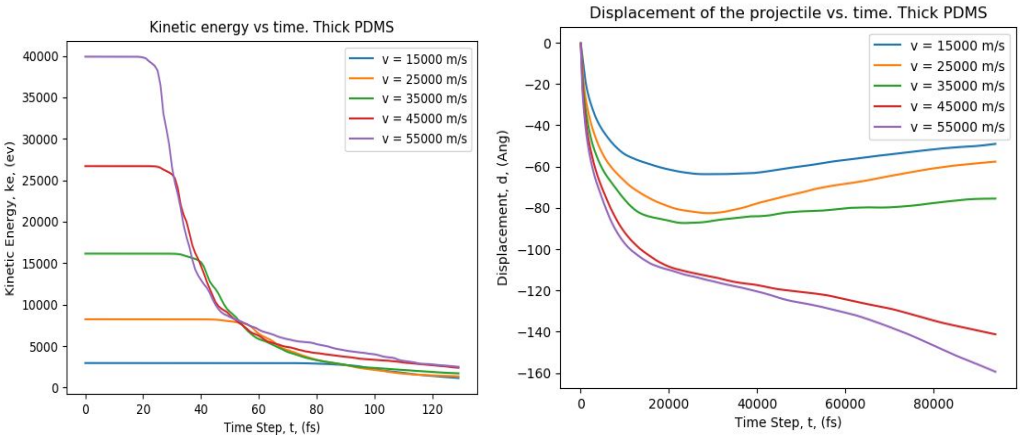

Figure 9: Projectile's kinetic energy and displacement time history for thick PDMS subjected to a projectile with different initial velocities

Aforementioned we recognized that the PDMS thickness plays an important role in bulletproofing especially when the graphene layers are embedded in between bulk of PDMS. However, looking more precisely on the kinetic energy time history it could be seen not only the thickness of PDMS contributes to the resistance of composite subjected to bullet, but also the initial velocity that bullet inters the PDMS plays an important role. To simulate the movement of the projectile inside the PDMS, a thick bulk PDMS model

(79.13×54.13×58 A in x, y, and z directions respectively) has been constructed. Then it is replicated in the x-direction with a 4.5 A distance between bulks models during replication. A python code has been developed to build a bullet with 20 A diameter, the same as before, and whole the construction is introduced in LAMMPS for further analysis. The bullets with different initial velocities start to move in the negative direction of the x-axis toward the PDMS and then hits it at the center. The kinetic energy and displacement time history are plotted in Fig. 9. It could be seen for the two initial velocities, 15000 and 25000 m/s, the bullet enters PDMS, get to a maximum displacement where the kinetic energy becomes zero, then the PDMS pushes it back and it moves backward some distance and traps inside the PDMS. When the initial velocity is around 35000 m/s the bullet reaches maximum displacement and kinetic energy become zero but does not move back and remains there. For the higher velocities, 45000 and 55000 m/s, the bullet moves through PDMS and complete perforation happens. Although, in this case, the difference between initial velocities are high, 10000 m/s, the bullet exits PDMS with the nearly same kinetic energy. It states a decrease in kinetic energy during impact strongly depends on the value of initial velocity. The higher initial velocity, the kinetic energy fells down more sharply.

To appreciate the relation between a decrease in kinetic energy and initial velocity let consider a moving object inside a gas or a fluid media. When a moving object (diamond ball) passes through a viscous media (PDMS), it experiences resistive forces via the media. In general, the resistive force could be written as follows:

$$F_{res} = -(k_1 v + k_2 v^2)\hat{v} \tag{1}$$

In Eq. (1) the first term in the right-hand side is called viscous term and the second one is called pressure term. $\hat{v}$ is unite vector and the minus sign states the resistive force is in the opposite direction of the speed. Furthermore, the resistive force applied on the bullet is represented by k_1, and k_2 which are depend on the kind of medium that the bullet passes through. Generally, the resistive force depends on the shape of the object, the size of the object, the medium that objects moving through, and the speed of the object. In this paper the object is considered to be a sphere and consequently the magnitude of the resistance force in the Eq. (1) can be written as:

$$|F_{res}| = c_1 r v + c_2 r^2 v^2 \tag{2}$$

Where C_1 and C_2 are constant with the dimensions of kg/m.s and Kg/m^3, respectively and r is the radius of the object. The viscous term is because of the stickiness of the medium that it is referred to as viscosity. If the medium is very sticky or has a high viscosity, the constant C_1 is very high. By looking at Eq. (2) it is seen that the pressure term is a function of the square radius r and bullet's velocity v. Since the radius is very small and the maximum velocity which is considered here is high, makes the pressure term is considerably lower than viscous term. Therefore, the pressure could be ignored compared to the viscous term, and as a result, the magnitude of resistive force could be written just in terms of the viscous term as follows:

$$|F_{res}| = c_1 r v \tag{3}$$

From Eq. (3), it could be seen the resistance force depends on the stickiness of the media, radius of the projectile, and the value of the initial velocity of the projectile. The resistance force of bullet passing through PDMS versus time for different initial velocities is plotted in Fig. 10. From the graphs in Fig. 10, it could be concluded that PDMS, with a low density of 0.92 gr/cm^3 is a very high sticky material and its combination as an interface material l for graphene, a high bullet resistance composite could be produced.

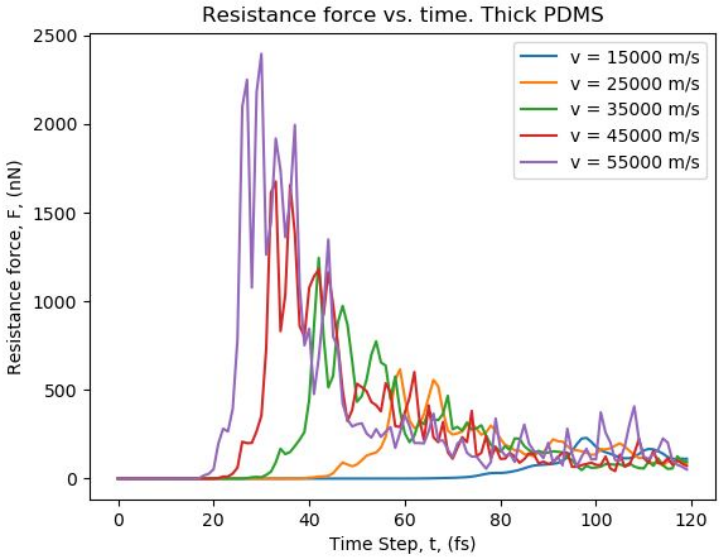

Figure 10: Resistance force applied by the PDMS to the projectile with different initial velocities

4 Concluding remarks

In this work we conducted extensive molecular dynamics simulations to explore the design of bulletproofing materials made of graphene and polydimethylsiloxane (PDMS). In order to comparatively explore different nanocomposite structures, PDMS polymers with three different thicknesses were constructed. In addition, single- or bi-layer graphene nanosheets were positioned either on the surface or in the middle of PDMS polymers. The constructed samples were then subjected to the impact by a spherical bullet made of diamond, with different initial velocities. The kinetic energy and displacement time history of the projectile for all models and different cases are plotted and compared accordingly. The results show as long as the graphene layers are embedded inside the PDMS, the composite resistance against bullet's penetration increases. Generally, it is shown that the thickness of PDMS, the number of graphene layers, and their position inside the PDMS contribute strongly to the bulletproofing response.

Authorship and Contribution: Timon Rabczuk[8, 9, *], Bohayra Mortazavi[2, 3], and Xiaoying Zhuang[2, 3] devised the project, and verified computational process and also

contributed to the final version of the manuscript. Alessandro Di Pierro[4], Emad Jomehzadeh[5], Zi Goangseup[6], and Kim Sang-Hyun[7] contributed in the simulation process. Hamidreza Nouri[1] worked out the technical details, and performed the computational calculations and wrote the manuscript.

Availability of Data and Materials: Supplementary materials data are available to download.

Funding Statement: B. M. and X. Z. appreciate the funding by the Deutsche Forschungsgemeinschaft (DFG, German Research Foundation) under Germany's Excellence Strategy within the Cluster of Excellence PhoenixD (EXC 2122, Project ID 390833453).

Conflicts of Interest: The authors declare that they have no conflicts of interest to report regarding the present study.

References

Abtew, M. A.; Boussu, F.; Bruniaux, P.; Loghin, C.; Cristian, I. (2019): Ballistic impact mechanisms-a review on textile and fiber-reinforced composites impact responses. *Composite Structures*, vol. 223, 110966.

Allen, M. P.; Tildesley, D. J. (1987): Computer simulation of liquids. *Oxford University Press*, New York.

Ammar, S.; Ramesh, K.; Vengadaesvaran, B.; Ramesh, S.; Arof, A. K. (2016): Amelioration of anticorrosion and hydrophobic properties of epoxy/PDMS composite coating containing nano ZnO particles. *Progress in Organic Coatings*, vol. 92, pp. 54-65.

Berdiyorov, G. R.; Mortazavi, B.; Ahzi, S.; Peeters, F. M.; Khraisheh, M. K. (2016): Effect of straining graphene on nanopore creation using Si cluster bombardment: a reactive atomistic investigation. *Journal of Applied Physics*, vol. 120, 225108.

Bizao, R. A.; Machado, L. D.; Sousa, J. M.; Pugno, N. M.; Galvao, D. S. (2018): Scale effects on the ballistic penetration of graphene sheets. *Scientific Reports*, vol. 8, pp. 1-8.

Brenner, D. W.; Shenderova, O. A.; Harrison, J. A.; Stuart, S. J.; Ni, B. et al. (2002): A second-generation reactive empirical bond order (REBO) potential energy expression for hydrocarbons. *Journal of Physics: Condensed Matter*, vol. 14, pp. 783-802**.**

Castaño M. V.; Rodríguez R. (2013), Nanotechnology for ballistic materials: from concept to products. *Materials and Technology*, vol. 47, pp. 267-271.

Chen, Z.; Xu, C.; Ma, C.; Ren, W.; Cheng, H. M. (2013): Light weight and flexible graphene foam composites for high-performance electromagnetic interface shielding. *Advanced Materials*, vol. 25, pp. 1296-1300.

Church, G.; Deamer, D. W.; Branton, D.; Baldarelli, R.; Kasianowics, J. (1998): Characterization of individual polymer molecules based on monomer-interface interactions. *US Patent,* Patent Number: 5,795,782.

Connor, C.; Chadwick, M. M. (1996): Characterization of absorbed water in aramid fiber by nuclear magnetic resonance. *Journal of Materials Science*, vol. 31, pp. 3871-3877.

D'Aloia, A. G.; Marra, F.; Tamburrano, A.; De Bellis, G.; Sarto, M. S. (2014): Electromagnetic absorbing properties of graphene-polymer composite shields. *Carbon*, vol. 73, pp. 175-184.

Edouk, U.; Faye, O.; Szpunar, J. (2017): Recent developments and applications of protective silicone coating: A review of PDMS functional material. *Progress in Organic Coating*, vol. 111, pp. 124-163.

Feng, D.; Aymerich, F. (2020): Effect of core density on the low-velocity impact response of foam-based sandwich composites. *Composite Structures*, vol. 239, pp. 112040.

Gama, B. A.; Chowdhury, S. C; Gillespie Jr, J. W. (2016): Molecular simulations of stress wave propagation and perforation of graphene sheets under transverse impact. *Carbon*, vol. 102, pp. 126-140.

Girish, T.; Tushar, T. H.; Shreenidhi, R. K. (2019): A review on integrants of polymer composites and its hybridization. *A Journal of Composition Theory*, vol. 7, pp. 124-128.

Izadifar, M.; Abadi, R.; Hossein Nezhad Shirazi, A.; Alajlan, N.; Rabczuk, T. (2018): Nanopores creation in boron and nitrogen doped polycrystalline graphene: a molecular dynamics study. *Physica E: Low-Dimensional System and Nanostructtures*, vol. 99, pp. 24-36.

Jassal, M.; Ghosh, S. (2002): Aramid fibers-an overview. *Indian Journal of Fiber & Textile Research*, vol. 27, pp. 290-306.

Jermann, M. (2015): Particle therapy statistics in 2014. *International Journal of Particle Therapy*, vol. 2, pp. 50-54.

Ji, X.; Xu, Y.; Zhang, W.; Cui, L.; Liu, J. (2016): Review of functionalization, structure and properties of graphene/polymer composite fibers. *Composites Part A: Applied Science and Manufacturing*, vol. 87, pp. 29-45.

Kakati, S.; Chakraborty, D. (2020): Delamination in GLARE laminates under low velocity impact. *Composite Structures*, vol. 240, 112083.

Kasianowic, J. J.; Brandin, E.; Barton, D.; Deamer, D. W. (1996): Characterization of individual polynucleotide molecules using a membrane channel. *Proceedings of the National Academy of Sciences USA*, vol. 93, pp. 13770-13773.

Knotek, O.; Bosserhoff, B.; Schrey, A. (1992): A new technique for testing the impact load of thin films: the coating impact test. *Surface and Coating Technology*, vol. 54/55, pp. 102-107.

Lee, J. H.; Loya, P. E.; Lou, J.; Thomas, E. L. (2014): Dynamic mechanical behavior of multilayer graphene via supersonic projectile penetration. *Science*, vol. 346, pp. 1092-1096.

Li, J.; Zhao, Y.; Hu, J.; Shu, L.; Shi, X. (2012): Anti-icing performance of a super hydrophobic PDMS/modified nano-silica hybrid coating for insulators. *Journal of Adhesion Science and Technology*, vol. 26, pp. 665-679.

Li, W.; Liang, L.; Zhao, S.; Xue, J. (2013): Fabrication of nanopores in a graphene sheet with heavy ions: A molecular dynamics study. *Journal of Applied Physics*, vol. 114, 234304.

Mohan, R.; Grosshans, D. (2016): Proton therapy-present and future. *Advanced Drug Delivery Reviews*, vol. 109, pp. 26-44.

Njoroge, J. L. (2013): Atomistic simulation of graphene-polyurethane nanocomposite for use in ballistic applications. *Doctoral dissertation, Texas A & M University*.

Parandoush, P.; Lin, D. (2017): A review on additive manufacturing of polymer-fiber composites. *Composite Structures*, vol. 182, pp. 36-53.

Plimpto, S. (1995): Fast parallel algorithms for short-range molecular dynamics. *Journal of Computational Physics*, vol. 117, pp. 1-19.

Schneider, G. F.; Kowalczyk, S. W.; Calado, V. E.; Pandraud, G.; Zandbergen, H. W. et al. (2010): DNA translocation through graphene nanopores. *Nano Letters*, vol. 10, pp. 3163-3167.

Stuart, S. J; Tutein, A. B; Harrison, J. A. (2000): A reactive potential for hydrocarbons with intermolecular interactions. *Journal of Chemical Physics*, vol. 112, pp. 6472-6486.

Stukowski, A. (2009): Visualization and analysis of atomistic simulation data with OVITO-the open visualization tool. *Modeling and Simulation in Materials Science and Engineering*, vol. 18, 015012.

Sun, H.; Rigby, D. (1997): Polysiloxanes: Ab initio force field and structural, conformational and thermophysical properties. *Spectrochimica Acta Part A: Molecular and Biomolecular Spectroscopy*, vol. 53, pp. 1301- 1323.

Sun, H. (1995): Ab initio calculations and force field development for computer simulation of polysiloxanes. *Macromolecules*, vol. 28, pp. 701-712.

Sun, H. (1998): CPMPASS: An ab initio force-field optimization for condensed-phase application-overview with details on alkane and benzene. *The Journal of Physical Chemistry B*, vol. 102, pp. 7338-7364.

Unnikrishnan, K. P.; Thachil, E. T. (2012): Toughening of epoxy resins. *Designed Monomers and Polymers*, vol. 9, pp. 129-152.

Wagih, A.; Sebaey, T. A.; Yudhanto, A.; Lubineau, G. (2020): Post-impact flexural behavior of carbon- aramid/epoxy hybrid composites. *Composite Structures*, vol. 239, 112022.

Wang, H.; Zhao, X.; He, C. (2016): Enhanced antifouling performance of hybrid PVDF ultrafiltration membrane with the dual-mode SiO_2-g-PDMS nanoparticles. *Separation and Purification Technology*, vol. 1, pp. 1-8.

Wasfi, A.; Awwad, F.; Ayesh, A. l. (2018): Graphene-based nanopro approaches for DNA sequencing: a literature review. *Biosensors & Bioelectronics*, vol. 119, pp. 191-203.

Wu, E.; Chang, L. C. (1995): Woven glass/epoxy laminates subjected to projectile impact. *International Journal of Impact Engineering*, vol. 16, pp. 607-619.

Yahaya, R.; Sapuan, S. M.; Jawaid, M.; Leman, Z.; Zainudin, E. S. (2016): Water absorption behavior and impact strength of Kenaf-Kevlar reinforced epoxy hybrid composites. *Advanced Composites Letters*, vol. 25, pp. 97-102.

Zee, R. H.; Hsieh, C. Y. (1998): Energy absorption process in fibrous composites. *Materials Science and Engineering: A*, vol. 246, pp. 161-168.

Zhang, D.; Sun, Y.; Chen, L.; Zhang, S.; Pan, N. (2014): Influence of fabric structure and thickness on the ballistic impact behavior of ultrahigh molecular weight polyethylene composite laminated. *Material & Design*, vol. 54, pp. 315-322.

Zhang, Y.; Mi, C. (2020): Strengthening bonding strength in NiTi SMA fiber-reinforced polymer composites through acid immersion and Nanosilica coating. *Composite Structures*, vol. 239, pp. 112001.

Zhao, Y. D; Xie, Y.; Liu, Z.; Wang, X.; Chai, Y. et al. (2014): Two-dimensional material membranes: An emerging platform for controllable mass transport applications. *Small*, vol. 10, pp. 4521-4542.

Zhu, G.; Goldsmith, W.; Dharan, C. K. H. (1992): Penetration of laminated Kevlar by projectiles. II: Analytical model. *International Journal of Solids and Structures*, vol. 29, pp. 421-436.